HHS Public Access

Author manuscript

*Wound Repair Regen*. Author manuscript; available in PMC 2018 July 05.

Published in final edited form as:

*Wound Repair Regen*. 2017 May ; 25(3): 443–453. doi:10.1111/wrr.12544.

# Level-Specific Amputations and Resulting Regenerative Outcomes in the Mouse Distal Phalanx

**Connie S. Chamberlain, PhD**[1], **Justin J. Jeffery, BS**[2], **Ellen M. Leiferman, DVM**[1], **Tugrul Yildirim, MD**[1], **Xin Sun, PhD**[4], **Geoffrey S. Baer, MD, PhD**[1], **William L. Murphy, PhD**[1,3], and **Ray Vanderby, PhD**[1,3]

[1]Department of Orthopedics and Rehabilitation, University of Wisconsin-Madison, Madison, Wisconsin 53705

[2]Department of Comprehensive Cancer Center, University of Wisconsin-Madison, Madison, Wisconsin 53705

[3]Department of Biomedical Engineering, University of Wisconsin-Madison, Madison, Wisconsin 53705

[4]Laboratory of Genetics, University of Wisconsin-Madison, Madison, Wisconsin 53705

**Keywords**

mouse digit regeneration; distal phalanx; amputation; blastema; histolysis

## Introduction

Regeneration is a complex process that typically results in growth, restoration, and renewal of the injured structure. All species from different evolutionary complexities possess some capacity to regenerate. However, the regenerative potential declines with the evolution of divergence. Hydra and planarians are tremendous regenerators, capable of restoring large regions of missing structures. The more structurally complex amphibians and newts are capable of regenerating limbs and tails. Mammalian limb regeneration also occurs but is limited to digit tips in humans, non-human primates, rats, and mice.(1–5) Thus, the digit tip provides a potentially important model to identify mechanisms of mammalian tissue regeneration.

Digit tip regeneration involves an intricate coordinated regrowth of the terminal phalanx, nail, dermis and epidermis. After amputation, regenerating digits undergo wound healing, blastema formation, and re-differentiation.(6) Wound healing, lasting up to 10 days in the adult mouse, is characterized by increased cell proliferation, histolysis, and the absence of wound closure.(6, 7) Histolysis is the process of ECM[1] degradation involved in cell release

**Corresponding Author:** Connie S. Chamberlain, Ph.D.: 1111 Highland Ave, WIMR Room 5059, Madison, WI 53705. Chamberlain@ortho.wisc.edu, phone: 608-265-0487; fax: 608-262-2989.

[15]MMP: matrix metalloproteinase

No competing financial interests exist.

[1]ECM: extracellular matrix

and may also promote blastema development.(8–13) The histolytic process is well-documented in the regenerating axolotl and is apparent within 2–3 days post-amputation in larval urodeles and within 4–5 days in adults.(14–16) As a result, tissues near the wound epidermis undergo intense degradation, via proteolytic digestion, for 1–2 mm. Histolysis has also been described in the mouse amputation model, and is associated with secondary bone loss to the bone marrow cavity.(6, 17, 18) Blastema formation initiates after the completion of wound closure.(6, 7) The blastema is a highly proliferative, undifferentiated mass of cells localized between the bone marrow cavity and distal bone stump that contributes to the regenerative process.(19) Differentiation of these cells initiates the process of bone rebuilding and is detectable by day 12–14 post amputation.(6, 19) Ossification of bone is first apparent at the bone stump interface and base of blastema, which results in direct intramembranous ossification. (6, 19) As previously reported, the general anatomy of the regenerating P3 is essentially restored by day 28 and by day 128 the digit tip is similar to the native digit.(6)

The capacity to regenerate the digit is dependent on the level of the amputation. Amputation less than 30% of the P3[2], with part of the base nail remaining, results in extensive (but not complete) regeneration.(2, 3, 6, 19) In contrast, over 60% P3 removal results in no regeneration.(3) This level-dependent regenerative ability of the mouse digit provides a comparative model between regeneration and non-regeneration that may enable identification of specific factors pertinent to regeneration. Although the ability to create a regenerating and non-regenerating condition by amputation of <30% or >60%, respectively, has been well established, the regenerative response between these regions (“intermediate” zones) has received less scrutiny, yet it may add insight to the regenerative processes. A previous study measuring the regrowth of amputated mouse digits within the intermediate zone reported both regenerative and non-regenerative outcomes.(3) These variations may have resulted from the lack of available technology to accurately measure the amount of bone originally amputated from these small samples (Fig. 1a). Elucidation of the level-specific amputations with specific focus on the intermediate area using the more precise microCT method to monitor the amount of bone amputated and subsequent regrowth will more clearly define the capacity for the digit to regenerate. Moreover, the ability to accurately measure *in vivo* regrowth of mouse digits across time will provide valuable insight into the regeneration cascade. The objective of this study is then to compare the regeneration capacity between amputation levels within the regenerating (<30%), intermediate (40–59%), and non-regenerating (>60%) regions.

## Methods

### Surgical procedure

All experiments were approved by the University of Wisconsin-Madison Institutional Animal Care and Use Committee. A total of eighteen 9–10 week old adult male C57Bl/6 mice were used for the study. Mice were subjected to bilateral hindlimb P3 amputation to digits 2, 3 or 4. For each amputation, mice were anesthetized, the hindlimb claw was

[2]P3: distal phalanx

extended, and the distal phalanx and footpad was sharply dissected. A regenerating distal phalanx was generated by amputating <30% of the P3 (n=5 mice). Intermediate digit amputations (n=5 mice) were created by removing 40–59% of the distal phalanx. A non-regenerating digit (n=5 mice) was created by amputating >60% of the P3 bone. Skin wounds were allowed to heal without suturing. A total of 50 digits were amputated for the microCT study to obtain a minimum number of 10 digits per group. Any digits that did not fall within the designated amputation guidelines were omitted from the study. Mice were subjected to microCT[3] imaging of the digits one day prior to surgery ("pre[4]"; to establish a baseline), immediately after amputation ("amp[5]"), then on day 5, 7, 14, 21, 26–28 (herein referred to as day 28), 35, 42, and 49–56 (herein referred to as day 56). Based on the microCT results indicating the percentage of bone removed, the number of regenerating, intermediate, and non-regenerating digits were 10, 19, and 16 digits, respectively. Another group of three mice were subjected to bilateral regenerating, intermediate, and non-regenerating digit amputations and sacrificed at 14 days post-amputation. Digits were fixed in 10% neutral buffered formalin, decalcified in 5% formic acid, paraffin-embedded and used for histology and immunohistochemistry.

## MicroCT Analysis

Mice hindlimb paws were longitudinally imaged using microCT to assess digit regeneration. MicroCT provides the necessary resolution and contrast to measure digit length and volume used in the analysis. Imaging was performed using a Siemens Inveon microCT scanner, and analysis was conducted using Inveon Research Workplace General and 3D Visualization software (Siemens Medical Solutions USA, Inc., Knoxville, TN). All scans were acquired with the following parameters: 80 kVp, exposure time, 900 μA current, 220 rotation steps with 441 projections, ~16.5 minute scan time, bin by 2, 50 micron focal spot size, and medium magnification that yielded an overall reconstructed isotropic voxel resolution of 46.6 μm. With a 46 μm digital isotropic voxel resolution, the full-width half-max (FWHM) is 46 μm. The FWHM is approximately 2.355 standard deviations, which means the standard deviation the digit measurements are approximately 19.53 μm, more than an order of magnitude smaller than mean differences. With a 95% confidence interval, differences of 38.28 μm between measurements can be detected.

Raw data were reconstructed with filtered back-projection and no down-sampling using integrated high-speed COBRA reconstruction software (Exxim Computing Corporation, Pleasanton, CA). HU[6], a scalar linear attenuation coefficient, was applied to each reconstruction to permit inter-subject comparisons. Three-dimensional images were segmented using a minimum pixel intensity of 300 HU, and a maximum intensity of 3168 HU to represent bone density. [40] After the region of interest was defined, the P3 volume was calculated. Sagittal length of the digits was also obtained by measuring twice from the distal tip to proximal edge of the P3 bone. Two researchers who were blinded to one another's measurements independently conducted analyses, and their results were averaged.

[3]microCT: micro-computed tomography
[4]Pre: pre-amputation
[5]Amp: amputation
[6]HU: Hounsfield units

### Immunohistochemistry (IHC) and Histological Analysis

In order to identify bone repair differences within the amputated digit, IHC and histology were performed. Sagittally positioned PET[7] were sectioned (5 μm thickness), and placed on Colorfrost Plus (Fisher Scientific, Pittsburgh, PA) slides. IHC[8] was performed on fixed, decalcified, deparaffinized sections using rabbit polyclonal antibodies. Sections were exposed to 3% hydrogen peroxide to remove endogenous peroxidase activity, fixed in 10% neutral buffered formalin to prevent removal of sections from slides, subjected to 80C heat-induced epitope retrieval using 10 mM sodium citrate buffer, blocked with 10% BSA/PBS[9] and incubated with polyclonal antibodies to Ki-67 (1:750; Cambridge, MA) to identify proliferating cells. Sections were then incubated with Rabbit on Mouse HRP polymer (Biocare Medical, Concord CA). The bound antibody was visualized using DAB[10]. Stained sections were dehydrated, cleared, cover-slipped and visualized using light microscopy. To detect osteoclasts, TRAP[11]staining (Sigma, St. Louis, MO) was performed. After staining, images of each IHC marker were collected using a camera -assisted microscope (Nikon Eclipse microscope, model E6000 with an Olympus camera, model DP79). Mouse digits were also H&E[12] stained to observe general morphology of the distal phalanx.

### Statistical Analysis

MicroCT results were averaged for each amputation group within each collection day, and metrics were subjected to ANOVA[13] to examine differences across time. If the overall p-value for the F-test in ANOVA was significant ($p < 0.05$), Tukey's post-hoc comparisons were performed. Proliferating cells were analyzed via Student's t-tests. Results were considered statistically significant if $p \leq 0.05$. Experimental results are presented as the means ± S.E.M.[14] Computations were performed using KaleidaGraph, version 4.03 (Synergy Software, Inc., Reading, PA).

## Results

### Defining the Regrowth Zones

To first identify and confirm level-specific bone regrowth zones after amputation, digits were separated into groups based on the percent of bone initially amputated from the original digit length and included 10–19%, 20–29%, 40–49%, 50–59%, 60–69%, and 70–79%. The percent of bone recovered was calculated by the amount of total bone removed (pre-amputation length minus day 14 length) and divided by the amount of bone regrown at day 56. Based on this metric, three groups (Fig 1b-c) were distinguishable: digits subjected to 1) regenerating amputations (10–19% and 20–29%), 2) intermediate amputations (40–49% and 50–59%) and 3) non-regenerating amputations (60–69% and 70–79%). Bone recovery was significantly different between these three groups. The greatest amount of bone was

[7]PET: paraffin-embedded tissue
[8]IHC: immunohistochemistry
[9]BSA/PBS: bovine serum albumin/phosphate buffered saline
[10]DAB: diaminobenzidine
[11]TRAP: tartrate resistant acid phosphatase
[12]H&E: hematoxylin and eosin Y
[13]ANOVA: analysis of variance
[14]SEM: standard error of the mean

recovered in digits initially amputated at 10–19% (88.86 ± 12.68%) and 20–29% (79.96 ± 8.61%; Fig. 1b-c). Amputation of 40–49% and 50–59% resulted in a recovery rate of 42.25 ± 6.62% and 44.05 ± 7.29% respectively. Non-regenerating amputations of 60–69% and 70–79% recovered 19.15 ± 7.93% and 8.56 ± 2.27%, respectively. Within each group levels were similar and subsequent data was sorted into amputations of <30%, 40–59%, and >60%.

## Development of Level-Specific Amputations

To confirm grouped level-specific amputations, all digits were subjected to microCT analysis before and after amputation. Prior to amputation, digits designated as "regenerating" (amputated <30%), "intermediate" (amputated 40–59%), and "non-regenerating" (amputated >60%) were 1.42 ± .02 mm, 1.52 ± .01 mm, and 1.49 ± .02 mm in length (Table 1). Volumes of intact digits were 0.20 ± .01 $mm^3$, .29 ± .01 $mm^3$ and .26 ± .01 $mm^3$ (Table 1). Post-amputation of the P3 bone to create regenerative, intermediate, and non-regenerative models resulted in the removal of 16.81 ± 1.53%, 49.65 ± 1.31%, and 69.92 ± 1.50% of the bone length, confirming appropriate regeneration models. Volume of the amputated digits resulted in the loss of 12.31 ± 2.50%, 32.70 ± 3.86%, and 56.5 ± 4.11% for the regenerating, intermediate, and non-regenerating digits, respectively (Table 1; Fig. 1). MicroCT images indicated that digits subjected to regenerating amputations retained the P3 bone marrow cavity immediately post amputation (Fig. 1). Intermediate amputations removed the distal P3 up to the bone marrow cavity (Fig. 1). Non-regenerating amputations removed the majority of the P3 bone, including the bone marrow cavity (Fig. 1).

## Comparison of Regrowth Using MicroCT Analysis

To further compare the injury outcomes, amputated digits were measured across time via microCT. Amputation of the distal phalanx to create non-regenerating digits (>60% P3 removed) resulted in no changes throughout the time analyzed: length and volume remained similar to the d0 amputated digits (Fig. 2). Amputation of the distal phalanx to create a regenerating scenario (<30% P3 removed) resulted in no significant difference in bone length and volume within the first 7 days after amputation. ($p < 0.05$; Fig. 3). By days 14 and 21 ($p < .0001$), digit histolysis was prevalent and resulted in significant bone loss beyond the original amputation plane (Fig 3e-f, k-l). Bone length and volume was effectively regained at day 28 and levels were similar to the time of amputation. From day 35 until the end of the study, bone regrowth was evident such that the length was similar to the pre-amputated state by day 56. Bone volume at day 42 in the regenerating group was significantly ($p < 0.05$) increased beyond its pre-amputated volume. Similar to the regenerating digits, the intermediate digits (40–59%) exhibited no significant change in length or volume the first 7 days post-amputation (Fig. 4). By day 14, histolysis was also evident within these digits (Fig. 4). Bone length increased after day 14. However, in contrast to the regenerating digits, bone re-growth did not approach pre-amputation values, indicating incomplete regeneration.

## Histolysis and Blastema Formation after Amputation

The aforementioned results indicate that histolysis was significant in both the regenerating and intermediate amputations, but regenerative outcomes were different. The extents of

blastema formation and histolysis were then compared between the amputated groups to discern any differences during the regenerative process. Day 14 H&E stained digit samples indicated blastema formation was evident in both the regenerating and intermediate amputations. Within the histolytic regions of the regenerating and intermediate digits, blastema formation was prominent and extended from the bone marrow cavity to the epidermis. Measurement of the blastema indicated no significant difference in size between the regenerating and intermediate digits (Fig. 5a-e). The non-regenerating digits likewise exhibited increased cellular activity at the distal P3 but lacked the prominent blastema found in the regenerating and non-regenerating digits ($p= 0.82$; Fig. 5a-e). The remaining P3 after histolytic shortening was measured (Fig. 5f). Interestingly, the size of the remaining distal phalanx, regardless of the regenerating outcome, was similar among all groups at day 14 ($p = .823$); the P3 was reduced to the base of the normally-shaped triangular bone, proximal to the marrow cavity. Because the P3 sizes were similar across groups, the amount of bone removed via histolysis was further compared. Although the amount of bone removed from the histolysis process was highest within the regenerating digit ($50.78 \pm 6.20$ mm), levels were statistically similar to the intermediate digits ($33.40 \pm 3.50$ mm; Fig. 5g). In contrast, the amount of bone removed at day 14 by the non-regenerating digit was significantly lower ($6.6 \pm 8.34$ mm) than the regenerating and intermediate digits. The amount of bone remaining at day 14 by the non-regenerating digit was not significantly different compared to amount remaining on the day of amputation (Fig. 2).

Regardless of the initial amount of bone removed across the three amputation groups the size of the P3 was similar at day 14. To further compare the extent of histolysis and resulting bone regrowth, digits were grouped according to the initial amount of bone amputated (10–19%, 20–29%, 40–49%, 50–59%, 60–69% and 70–79%). Figure 6a-b show the microCT compilation of digit regrowth across time after amputation. Remarkably, the digit length at day 14 was similar among all amputated groups over 19% despite the substantial differences in the initial level of amputation. However, the amount of new bone formed between day 14 and day 56 differed considerably depending on the initial amputation level. Only amputations of 10–19% resulted in less total bone removed (histolytic plus amputation), although the time to maximum histolysis was consistent with all amputation groups.

## Osteoclasts and Proliferating Cell Localization

Histolysis of the day 14 distal phalanx results in similar amounts of bone remaining, regardless of the initial amputation level (over 19%). These results suggest the degree of osteoclast-induced bone degradation may be different between the amputation levels. To determine osteoclast activity within the regenerating, intermediate, and non-regenerating digits, TRAP localization was analyzed (Fig. 7). The level of TRAP-positive osteoclasts was significantly higher in the intermediate P3 compared to the regenerating and non-regenerating digits. Overall, osteoclasts were primarily localized to the bone marrow cavity in the intact digit. Regenerating amputations resulted in TRAP localization around both the marrow cavity and areas of histolysis. Osteoclasts were also noted within the non-regenerating digit, at the distal edge of the P3 bone. Within the intermediate amputated digits, the number of TRAP-positive osteoclasts was significantly greater than all other groups, with cells dispersed throughout the bone marrow and distal phalanx.

To determine the degree of cell proliferation within the digit blastema and P3, day 14 samples were stained with Ki67, a marker for cell proliferation. Proliferating cells within the intact digit were primarily localized to the nail bed, ventral fat pad, and epidermal lining (Fig. 8). Within the regenerating digit, proliferating cells were mostly localized within the blastema. The intermediate digit exhibited an increase in proliferating cells compared to the intact ($p = 0.008$) and regenerating ($p = 0.08$) digits. Cells within the intermediate digit were dispersed throughout the blastema and region near the bone marrow cavity. The non-regenerating digits demonstrated variable levels of proliferating cells between samples and were not significantly different among the groups. The variable cell proliferation levels within non-regenerating digits appeared to be based on the level of P3 remaining. The most extreme amputations resulted in few proliferating cells, whereas the digits with more bone remaining displayed more proliferating cells.

## Discussion

Literature indicates that the ability to regenerate the distal phalanx is dependent on the initial level of amputation: removal of <30% or >60% of the distal phalanx results in regeneration-competent and regeneration-incompetent digits, respectively.(2, 3, 6, 19, 20) However, the post-amputation behaviors within the “intermediate” zone (40–59% amputated) are typically not discussed. This omission makes regeneration appear to be a bimodal function of amputation length. To our knowledge, this is the first report to compare the *in vivo* regenerating behaviors of the regenerative, intermediate, and non-regenerative amputations across time. Using microCT to measure bone length before and after digit amputation, we were able to precisely amputate digits to known levels, monitor bone re-growth *in vivo*, and identify level-specific bone recovery length within the regenerative (<30%), intermediate (40–59%), and non-regenerative amputation planes (>60%). MicroCT and histology results of the regenerative (< 30%) and intermediate amputations (40–59%) also indicated significant histolysis and blastema formation of the distal phalanx 14 days post-amputation. However, unlike the regenerating digits, intermediate amputations led to incomplete regrowth that did not approach levels of the intact digits. Non-regenerating amputations (>60%) did not exhibit significant histolysis or blastema formation. Remarkably, the histolytic process resulted in day 14 distal phalanges that were similar in length regardless of the initial amputation over 19%. The differences in histolysis, blastema formation and injury outcomes were also marked by changes in the number of proliferating cells and osteoclasts. Altogether, results indicate that although intermediate amputations result in histolysis and blastema formation similar to regenerating digits, the resulting cellular composition of the blastema differs, contributing to an incomplete regeneration.

MicroCT provides a sufficiently accurate method to monitor regrowth of the distal phalanx after amputation across time within the same animal. Previous reports have monitored digit regrowth using microCT after amputation. Those studies demonstrated the histolytic process between days 7 and 12 by the regenerating distal phalanx.(6, 7, 17, 21) However, they were restricted to bone regrowth of digits subjected to regenerative amputations. Our studies longitudinally compared bone regrowth of digits subjected to regenerating, intermediate, or non-regenerating amputations. The same mouse digits were monitored *in vivo* via microCT across time to more accurately reflect the regrowth process. Results from these comparative

longitudinal studies demonstrate that three level-specific amputations produce three different responses in histolysis, blastema formation, cellular profiles, and injury outcomes.

The regenerative process undergoes wound healing, blastema formation, and re-differentiation and results in a structure that recapitulates its native configuration. Histolysis and blastema formation were evident within the regenerating and intermediate digit amputations. Unlike the regenerating digits, the intermediate digits exhibited incomplete regeneration, suggesting the presence of histolysis and blastema formation does not predict a regenerative outcome. The histolysis results agree with Simkin et al., (2013) who reported that P2 amputations also undergo histolysis but do not regenerate.(7) Previous reports also indicated loss of 50% terminal phalanx during histolysis allows epidermal closure over the remaining bone or exposes marrow-derived stem cells to the injury.(6, 17, 18) We noted similar levels of histolysis-induced bone loss by the regenerating digit but bone loss was also evident in intermediate digits where the bone marrow cavity was opened with amputation, suggesting a role beyond exposing marrow-derived cells to the injury. The functional role of histolysis after amputation remains to be elucidated, but a similar process of secondary injury is also exhibited during wound healing in other models (e.g. injured tendon and ligament).(22–26) Wound healing by these models is characterized by granulation tissue that enlarges beyond the original confines of the injury to result in a larger more disorganized region that remodels to form scar. The histolysis/degradation mechanism resulting in blastema formation and regeneration rather than granulation tissue and scar formation requires further examination but appears to play a critical role in both the wound healing/regenerative response.

Immunohistochemistry results in this study demonstrated a significant increase in osteoclasts and proliferating cells by day 14 in the intermediate amputation digits. Osteoclasts function in bone remodeling to degrade bone matrix during histolysis while proliferating cells localize within the developing blastema. In our study the percent of bone lost via histolysis was statistically similar between the regenerating and intermediate digits, but the numbers of day 14 osteoclasts were different. Likewise, blastema formation was similar between the 2 amputation groups, but proliferating cells were higher in the intermediate group. The discrepancy in cell number between the two amputation groups may be attributed to both the time of tissue collection and the degree of injury to the digit. By day 14 the regenerating digit underwent significant histolysis and possibly, blastema formation. Thus the number of osteoclasts and proliferating cells may have maximized and diminished by the time of collection. Indeed, Fernando et al, (2011) reported an increase in osteoclasts by day 7 and a decrease by day 10 in the regenerating digit.(6) Within the regenerating digit, blastema formation was also reported to occur as early as 8 days post amputation, further supporting the earlier appearance of cells compared to the intermediate digits. The larger injury created by the intermediate amputations, relative to the regenerating digit, may have also protracted the regenerative process, corroborating the day 14 upregulation of cells and the day 56 incompletion of digit regeneration. Amputations to create a non-regenerating digit were the largest injury created but did not exhibit the same upregulation of osteoclasts as the intermediate amputations. Non-regenerating amputations resulted in the removal of the bone marrow cavity and an important source of osteoclasts needed for regeneration, possibly explaining the discrepancy of osteoclast number between the intermediate and non-

regenerating digits. The removal of regenerative signals via non-regenerating amputations may have also precluded the need to upregulate osteoclasts, rebuild bone and regenerate the digit. Altogether, amputation of the distal phalanx to generate three regenerative/reparative outcomes differentially modulated the number of proliferating cells and osteoclasts localized within the amputated digit, which may be attributed to the time of sample collection and the extent of injury at amputation.

The results from this study suggest regeneration outcomes are not directly based on the presence of histolysis and blastema formation, but rather, the retention of specific cells and/or signaling mechanisms within the regenerating zone of the amputated digit. Previous reports suggest that the nail plate must remain on the digit in order for successful regeneration.(3, 27) More recently, the presence of nail stem cells and activation of canonical Wnt signaling within the proximal nail matrix have been identified as critical regulators of regeneration.(3, 27, 28) Riginelli et al. (1995) report the regenerative ability of neonatal mouse digits is restricted to levels where the amputation plane is within the *Msx1* positive nail bed.(29) Altogether, the combination of signaling factors required for inducing regeneration are unknown, although the critical level of amputation to induce a regenerative response has been well established.

In conclusion, mouse distal phalanx amputations undergo a level-specific (but not binary) regeneration response. The combined total loss of bone resulting from the initial amputation and histolysis process, results in a similar sized digit at day 14, regardless of the future regenerative outcome. Amputations within an intermediate zone results in incomplete regeneration but are grossly similar in blastema formation and histolysis compared to regenerating digits. The difference in regeneration outcome between intermediate and regenerating digits is more predictive by the cellular profiles. Removal of the bone marrow cavity via non-regenerative amputations results in no regrowth of the digit, and partial removal with intermediate amputations results in an attenuated regenerative response. Altogether, these results suggest that the bone marrow cavity provides critical support to advance regeneration in the distal phalanx.

## Acknowledgments

The authors acknowledge Scott Liegel, Lia Woods, Katie M. Swift, Ben Kerzner, Kelsey A. Martin, and Bryan J. Roberts, for processing CT images and/or performing immunohistochemistry, Drew Roennenburg for digit processing, and the University of Wisconsin Small Animal Imaging Facility (SAIF). Authors would also like to acknowledge Reinier Hernandez and Frank Ranallo, PhD for microCT consultation. Research reported in this publication was supported by the AO Foundation under Award Number MSN161649 and the National Institute of Arthritis and Musculoskeletal and Skin Diseases of the National Institutes of Health under Award Number AR059916. The content is solely the responsibility of the authors and does not necessarily represent the official views of the AO Foundation or the National Institutes of Health.

## References

1. Illingworth CM. Trapped fingers and amputated finger tips in children. Journal of pediatric surgery. 1974; 9(6):853–58. [PubMed: 4473530]
2. Borgens RB. Mice Regrow the Tips of Their Foretoes. Science. 1982; 217(4561):747–50. [PubMed: 7100922]

3. Neufeld DA, Zhao W. Bone regrowth after digit tip amputation in mice is equivalent in adults and neonates. Wound repair and regeneration : official publication of the Wound Healing Society [and] the European Tissue Repair Society. 1995; 3(4):461–6.
4. Singer M, Weckesser EC, Geraudie J, Maier CE, Singer J. Open finger tip healing and replacement after distal amputation in rhesus monkey with comparison to limb regeneration in lower vertebrates. Anatomy and embryology. 1987; 177(1):29–36. [PubMed: 3439635]
5. Said S, Parke W, Neufeld DA. Vascular supplies differ in regenerating and nonregenerating amputated rodent digits. The anatomical record Part A, Discoveries in molecular, cellular, and evolutionary biology. 2004; 278(1):443–9.
6. Fernando WA, Leininger E, Simkin J, Li N, Malcom CA, Sathyamoorthi S, et al. Wound healing and blastema formation in regenerating digit tips of adult mice. Developmental biology. 2011; 350(2): 301–10. [PubMed: 21145316]
7. Simkin J, Han MJ, Yu L, Yan MQ, Muneoka K. The Mouse Digit Tip: From Wound Healing to Regeneration. Wound Regeneration and Repair: Methods and Protocols. 2013; 1037:419–35.
8. Weiss C, Rosenbau Rm. Histochemical Studies on Cell Death, Histolysis during Regeneration.I. Distribution of Acid Phosphomonoesterase Activity in Normal Regenerating and Resorbing Forelimb of Larval Spotted Salamander Amblystoma Maculatum. J Morphol. 1967; 122(3):203. [PubMed: 6050066]
9. Kato T, Miyazaki K, Shimizu-Nishikawa K, Koshiba K, Obara M, Mishima HK, et al. Unique expression patterns of matrix metalloproteinases in regenerating newt limbs. Developmental dynamics : an official publication of the American Association of Anatomists. 2003; 226(2):366–76. [PubMed: 12557215]
10. Miyazaki K, Uchiyama K, Imokawa Y, Yoshizato K. Cloning and characterization of cDNAs for matrix metalloproteinases of regenerating newt limbs. Proceedings of the National Academy of Sciences of the United States of America. 1996; 93(13):6819–24. [PubMed: 8692902]
11. Vinarsky V, Atkinson DL, Stevenson TJ, Keating MT, Odelberg SJ. Normal newt limb regeneration requires matrix metalloproteinase function. Developmental biology. 2005; 279(1):86–98. [PubMed: 15708560]
12. Yang EV, Gardiner DM, Carlson MR, Nugas CA, Bryant SV. Expression of Mmp-9 and related matrix metalloproteinase genes during axolotl limb regeneration. Developmental dynamics : an official publication of the American Association of Anatomists. 1999; 216(1):2–9. [PubMed: 10474160]
13. Yang EV, Bryant SV. Developmental regulation of a matrix metalloproteinase during regeneration of axolotl appendages. Developmental biology. 1994; 166(2):696–703. [PubMed: 7813787]
14. Neufeld DA. Bone Healing after Amputation of Mouse Digits and Newt Limbs - Implications for Induced Regeneration in Mammals. Anatomical record. 1985; 211(2):156–65. [PubMed: 3977084]
15. Hay ED, Fischman DA. Origin of the blastema in regenerating limbs of the newt Triturus viridescens. An autoradiographic study using tritiated thymidine to follow cell proliferation and migration. Developmental biology. 1961; 3:26–59. [PubMed: 13712434]
16. Thornton CS. Amphibian limb regeneration. Advances in morphogenesis. 1968; 7:205–49. [PubMed: 4881307]
17. Sammarco MC, Simkin J, Fassler D, Cammack AJ, Wilson A, Van Meter K, et al. Endogenous Bone Regeneration Is Dependent Upon a Dynamic Oxygen Event. J Bone Miner Res. 2014; 29(11):2336–45. [PubMed: 24753124]
18. Sammarco MC, Simkin J, Cammack AJ, Fassler D, Gossmann A, Marrero L, et al. Hyperbaric Oxygen Promotes Proximal Bone Regeneration and Organized Collagen Composition during Digit Regeneration. PloS one. 2015; 10(10):e0140156. [PubMed: 26452224]
19. Han M, Yang X, Lee J, Allan CH, Muneoka K. Development and regeneration of the neonatal digit tip in mice. Developmental biology. 2008; 315(1):125–35. [PubMed: 18234177]
20. Han M, Yang X, Farrington JE, Muneoka K. Digit regeneration is regulated by Msx1 and BMP4 in fetal mice. Development. 2003; 130(21):5123–32. [PubMed: 12944425]
21. Simkin J, Sammarco MC, Dawson LA, Tucker C, Taylor LJ, Meter KV, et al. Epidermal closure regulates histolysis during mammalian (Mus) digit regeneration. Regeneration. 2015; 2(3):106–18. [PubMed: 27499872]

22. Chamberlain CS, Crowley E, Vanderby R. The spatio-temporal dynamics of ligament healing. Wound Repair and Regeneration. 2009; 17(2):206–15. [PubMed: 19320889]

23. Chamberlain CS, Leiferman EM, Frisch KE, Wang SJ, Yang XP, Brickson SL, et al. The influence of interleukin-4 on ligament healing. Wound Repair and Regeneration. 2011; 19(3):426–35. [PubMed: 21518087]

24. Chamberlain CS, Leiferman EM, Frisch KE, Wang SJ, Yang XP, van Rooijen N, et al. The influence of macrophage depletion on ligament healing. Connective tissue research. 2011; 52(3): 203–11. [PubMed: 21117894]

25. Chamberlain CS, Leiferman EM, Frisch KE, Duenwald-Kuehl SE, Brickson SL, Murphy WL, et al. Interleukin-1 receptor antagonist modulates inflammation and scarring after ligament injury. Connective tissue research. 2014; 55(3):177–86. [PubMed: 24649870]

26. Chamberlain CS, Leiferman EM, Frisch KE, Brickson SL, Murphy WL, Baer GS, et al. Interleukin Expression after Injury and the Effects of Interleukin-1 Receptor Antagonist. PloS one. 2013; 8(8)

27. Mohammad KS, Day FA, Neufeld DA. Rapid communications - Bone growth is induced by nail transplantation in amputated proximal phalanges. Calcified Tissue Int. 1999; 65(5):408–10.

28. Takeo M, Hale CS, Ito M. Epithelium-Derived Wnt Ligands Are Essential for Maintenance of Underlying Digit Bone. The Journal of investigative dermatology. 2016; 136(7):1355–63. [PubMed: 27021406]

29. Reginelli AD, Wang YQ, Sassoon D, Muneoka K. Digit tip regeneration correlates with regions of Msx1 (Hox 7) expression in fetal and newborn mice. Development. 1995; 121(4):1065–76. [PubMed: 7538067]

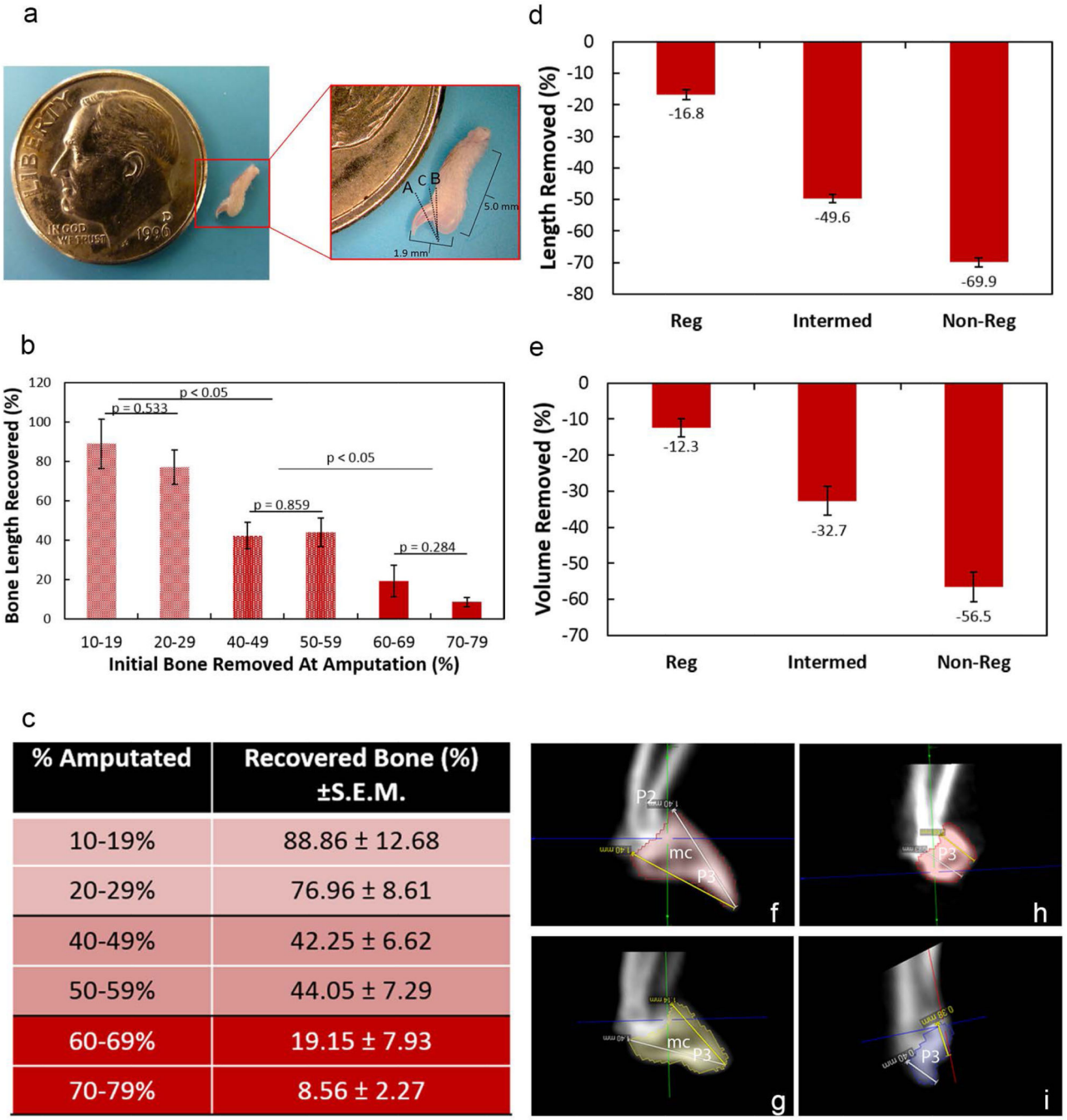


| % Amputated | Recovered Bone (%) ±S.E.M. |
|---|---|
| 10-19% | 88.86 ± 12.68 |
| 20-29% | 76.96 ± 8.61 |
| 40-49% | 42.25 ± 6.62 |
| 50-59% | 44.05 ± 7.29 |
| 60-69% | 19.15 ± 7.93 |
| 70-79% | 8.56 ± 2.27 |

**Figure 1. Level of bone removed to create regenerating and non-regenerating digits**

Representative example of a mouse hindlimb digit (a). The uppercase letters indicate the approximate regions of amputation to create a regenerating (A), non-regenerating (B) and intermediate (C) scenario. The amputated regions result in significant differences in bone length recovery (b–c). Digits were amputated at 10–19%, 20–29%, 40–49%, 50–59%, 60–69% and 70–79%. From these amputations, three different regions of bone recovery were identified within the regenerating (10–19% and 20–29%), intermediate (40–49% and 50–59%) and non-regenerating (60–69% and 70–79%) areas. Bone length (d), and bone volume

(e) of the mouse digit tip to create a regenerating, intermediate, and non-regenerating scenario. MicroCT 2D images of the mouse digits before and after amputation (f–i). The intact distal phalanx is comprised of a triangular-shaped bone (P3) containing a bone marrow cavity (m.c.) as indicated via microCT (f). Amputation to generate a regenerating digit resulted in the removal of bone distal to the bone marrow cavity (g). Intermediate amputations resulted in removal of bone up to the bone marrow cavity (h). In contrast, an amputation to create a non-regenerating digit resulted in removal of bone proximal to the bone marrow cavity (i). The pink (f–h), yellow (g), and purple (i) colors indicates the P3. Data are expressed as mean percent removed/recovered ± S.E.M. Significance was based on $p < 0.05$. P2: P2 phalanx; mc: marrow cavity; P3: distal phalanx.

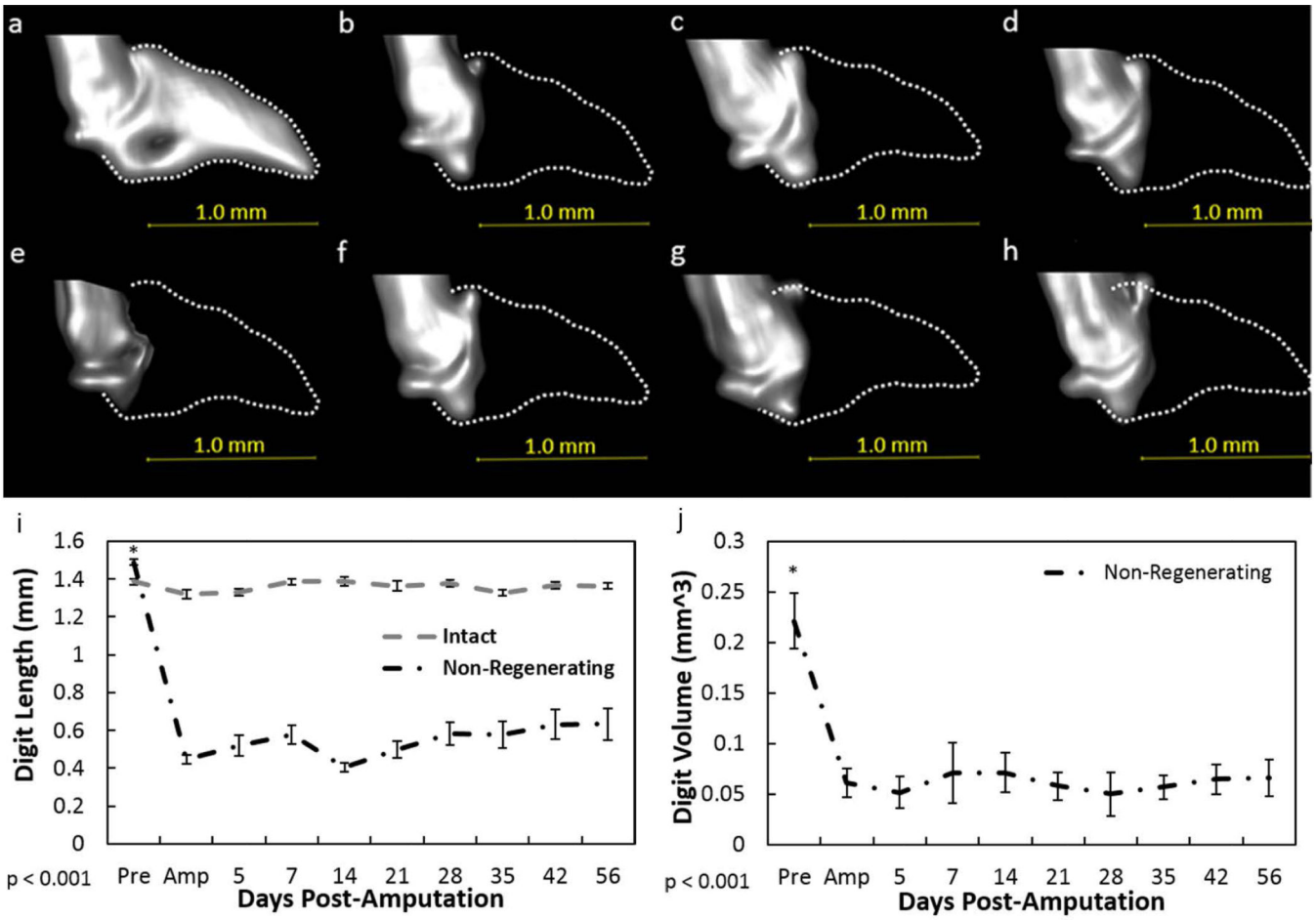


**Figure 2. MicroCT analysis of the non-regenerating digit**

Representative longitudinal 3D reconstructed microCT images of the non-regenerating digit before amputation (a), day of amputation (b), 7(c), 14 (d), 21 (e), 28 (f), 35 (g), 42(h) post-amputation from one selected animal. The dotted lines (a–h) indicate the original P3 shape. A non-regenerative amputation resulted in a significant decrease in bone length (i), and volume (j) which was not recovered over time. Data for the intact digit included in the 3 graphs were not factored into the statistics and only used as a visual baseline marker. Beneath graphs (i–j), p value indicates ANOVA results. Data are expressed as mean ± S.E.M. *indicates significance between pre-amputation and all post-amputation days as a result from Tukey's post-hoc pairwise comparisons where significance is $p < 0.05$.

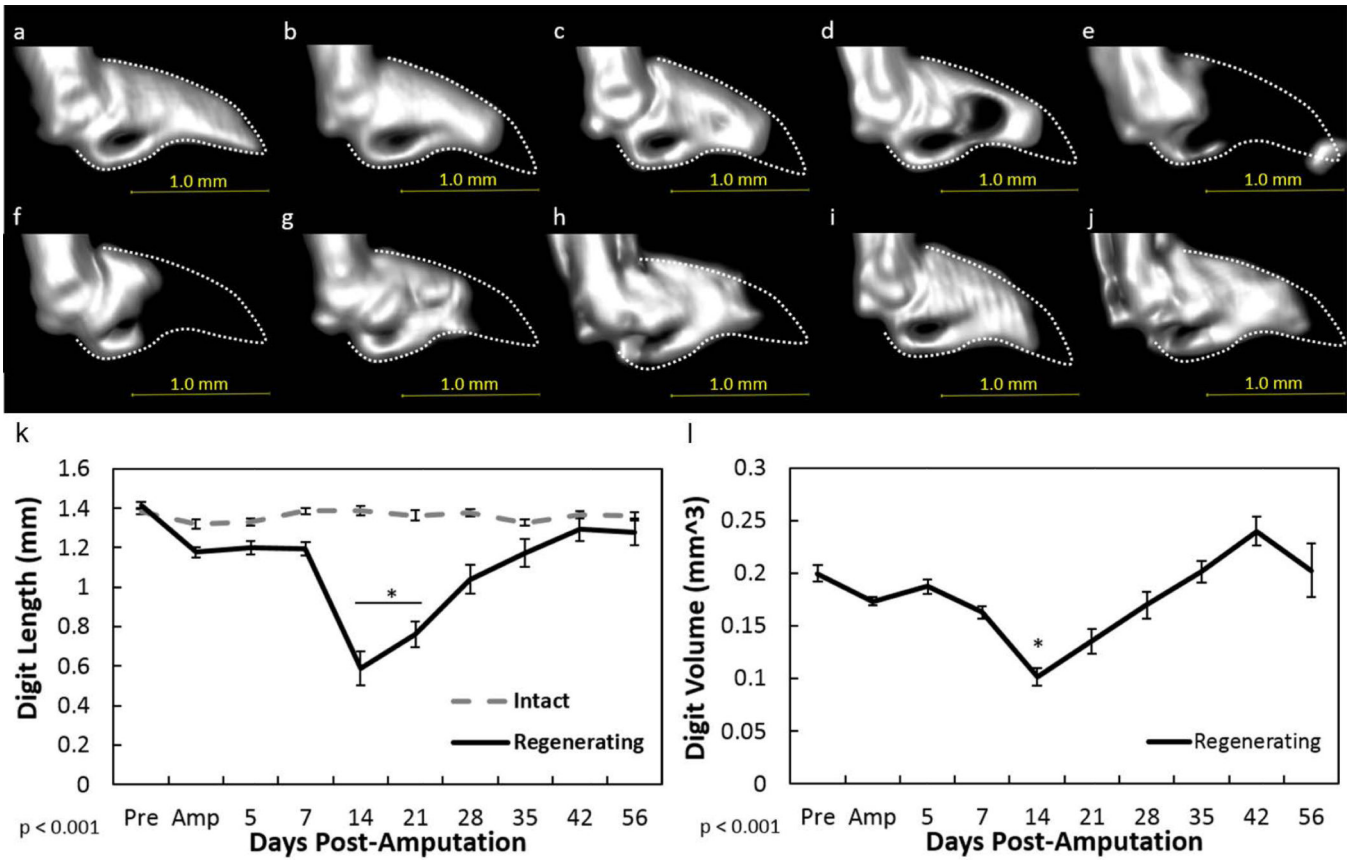


**Figure 3. MicroCT analysis of the regenerating digit**

Representative longitudinal 3D reconstructed microCT images of the regenerating digit before amputation (a), day of amputation (b), 5(c), 7 (d), 14 (e), 21 (f), 28 (g), 35 (h), 42 (i), and 56 (j) post-amputation from one selected animal. The dotted lines (a–j) indicate the original P3 shape before amputation. A regenerative-induced amputation resulted in a small reduction of bone length (k) and volume (l) on the day of amputation. However, a significant reduction in length and volume during histolysis was evident at day 14. Volume remained low at day 21. Thereafter, length and volume increased such that by day 56, levels were similar or greater than the length and volume pre-amputation values, respectively. Data for the intact digit included in the graph (k) were not factored into the statistics and only used as a visual baseline marker. Beneath graph, p value indicates ANOVA results. Data are expressed as mean ± S.E.M. *indicates significance at day 21 (k) and/or day 14 (k–l) between all other times. Significance is based on results from Tukey's post-hoc pairwise comparisons where significance is $p < 0.05$.

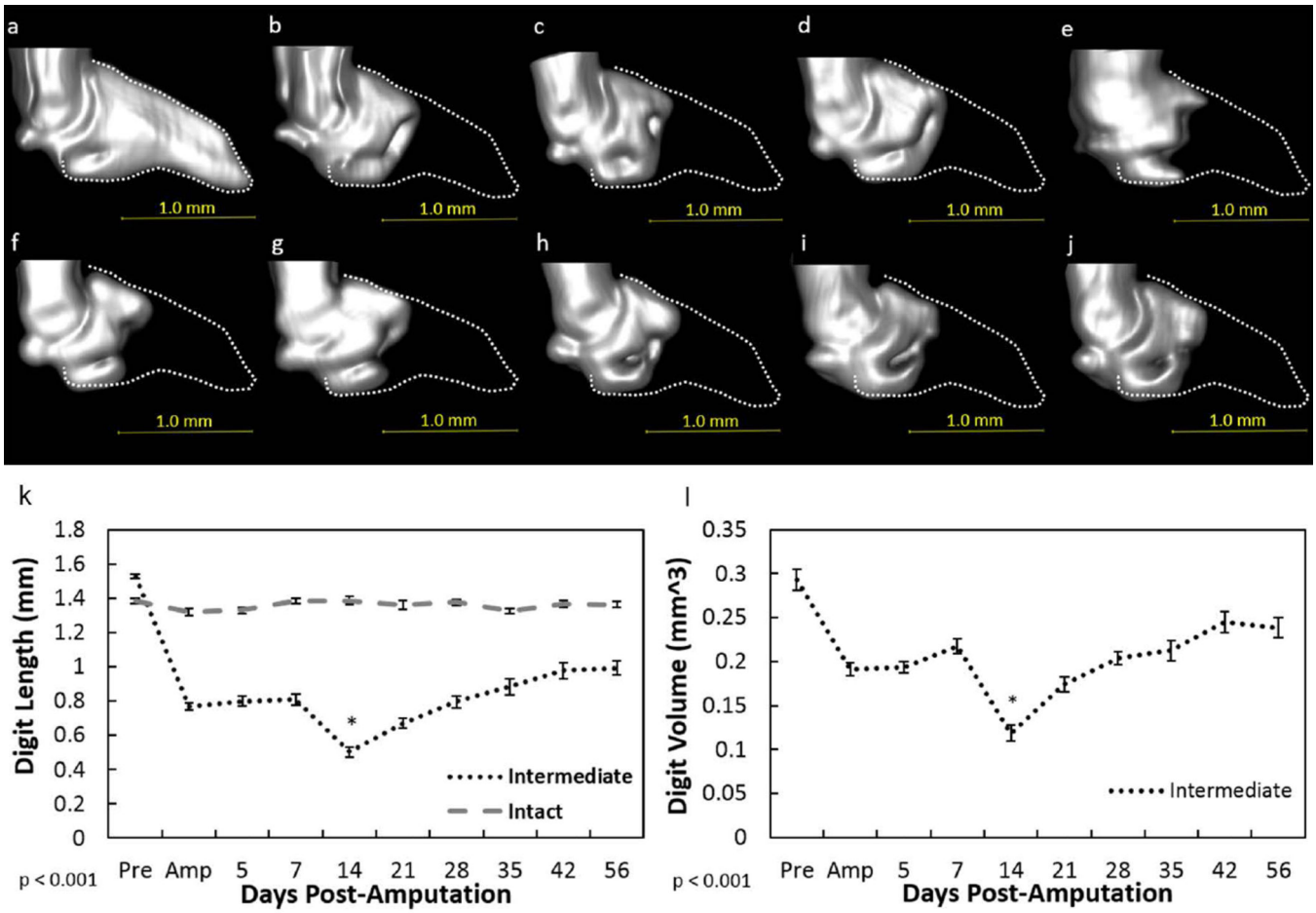


**Figure 4. MicroCT analysis of the intermediate digit**

Representative 3D reconstructed microCT images of the intermediate digit before amputation (a), day of amputation (b), 5(c), 7 (d), 14 (e), 21 (f), 28 (g), 35 (h), 42 (i), and 56 (j) post-amputation. The dotted lines (a–j) indicate the original P3 shape before amputation. An intermediate amputation resulted in a reduction of bone length (k) and volume (l) on the day of amputation. However, a significant reduction in length and volume during histolysis was evident at day 14. Thereafter, length and volume increased to reach day of amputation values. Data for the intact digit included in the graph (k) were not factored into the statistics and only used as a visual baseline marker. Beneath graph, p value indicates ANOVA results. Data are expressed as mean ± S.E.M. *indicates significance at day 14 (k–l) between all other times. Significance is based on results from Tukey's post-hoc pairwise comparisons where significance is $p < 0.05$. Pink color indicates P3.

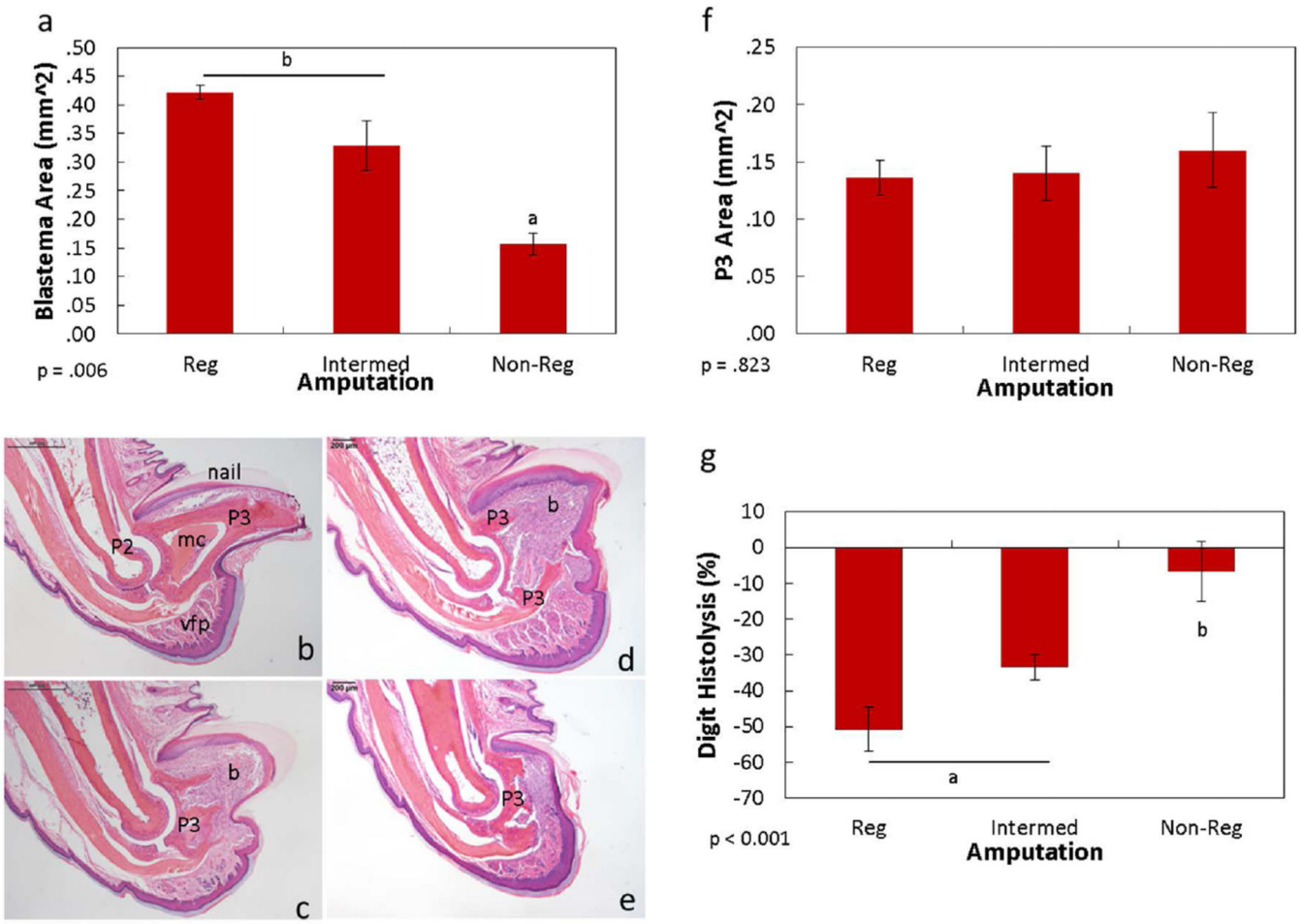


**Figure 5. Day 14 comparisons of histolysis and blastema formation between different regenerating outcomes**

Size of the day 14 blastema between regenerating and intermediate amputations were similar; non-regenerating digits were significantly smaller (a). Representative H&E images of the intact (b), day 14 regenerating (c), intermediate (d), and non-regenerating (e) digits. The day 14 regenerating and intermediate digits resulted in apparent blastema formation distal to the P3. The non-regenerating digit also exhibited an increase in cell mass distal to the P3.Size of the day 14 P3 indicated no significant differences between the 3 groups (f). The percent of histolysis at day 14 was similar between the regenerating and intermediate digits, whereas the non-regenerating digit was significantly less (g). Data are expressed as mean ± S.E.M. Significance is based on results from Tukey's post-hoc pairwise comparisons where significance is $p < 0.05$. $^{a,b}$denote significant differences between groups. P2: P2 phalanx; mc: marrow cavity; P3: distal phalanx; vfp: ventral fat pad; b: blastema.

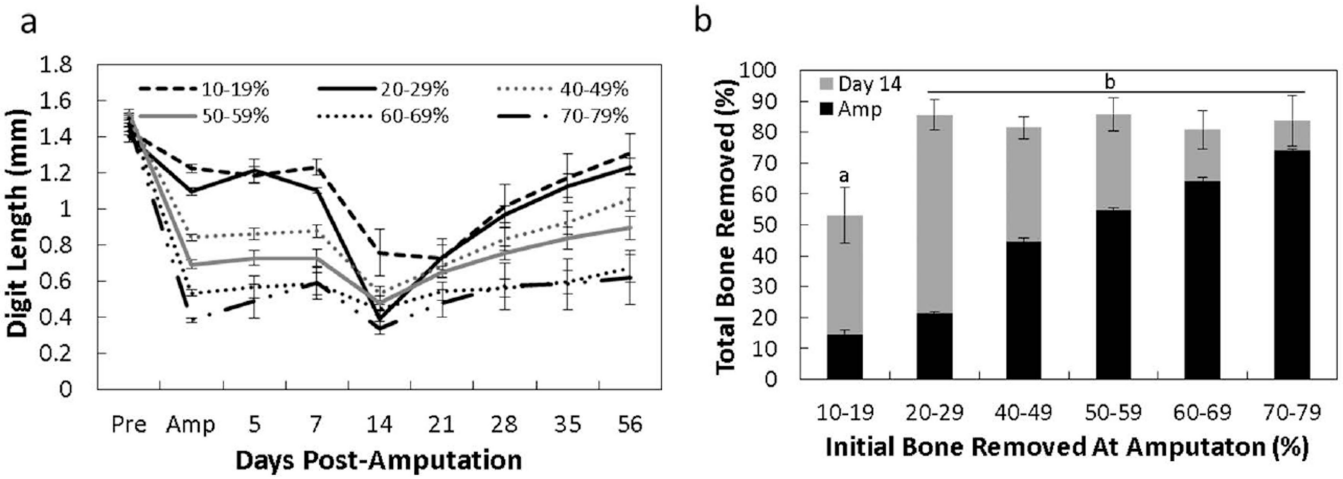


**Figure 6. Distal phalanx histolysis after amputations at different planes**

The amount of bone length remaining after histolysis is similar among groups, regardless of the initial amputation (a). The sum of total bone removed as determined by the initial amount of bone removed at amputation (black bars) and the amount of bone removed during the histolysis process (b; grey bars). The total bone removed was similar among digits with more than 19% bone removed. Significance is based on results from Tukey's post-hoc pairwise comparisons where significance is $p < 0.05$. [a,b]denote significant differences between groups.

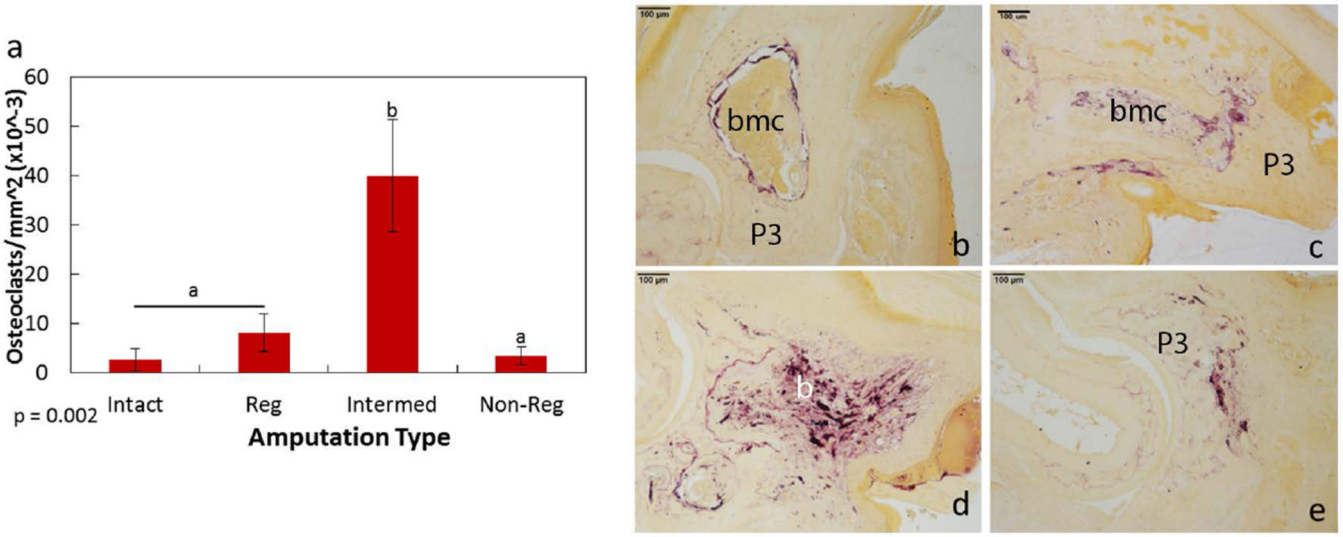


**Figure 7. Osteoclast localization within the day 14 amputated digits**

TRAP staining to identify osteoclasts indicated a significant increase in cells by the intermediate amputations when compared to the intact, regenerating and non-regenerating amputations (a). Representative images of TRAP staining by the intact (b), regenerating (c), intermediate (d), and non-regenerating (e) digits. Purple staining indicates TRAP-stained osteoclasts (b–e). Significance is based on results from Tukey's post-hoc pairwise comparisons where significance is $p < 0.05$. [a,b]denote significant differences between groups.

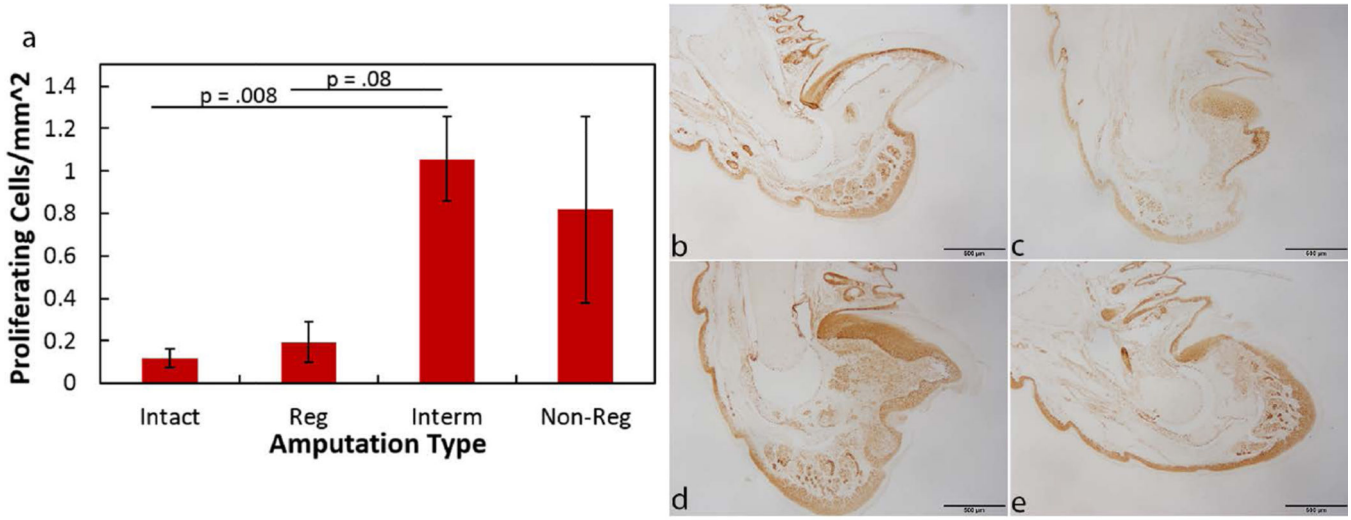


**Figure 8. Proliferating cells within the day 14 amputated digits**

Ki67 immunohistochemistry to identify proliferating cells indicated an increase in cells by the intermediate digits when compared to the intact and regenerating digits (a). Representative images of Ki67 immunohistochemistry by the intact (b), regenerating (c), intermediate (d), and non-regenerating (e) digits. Brown color indicates DAB staining of cells (b–e). Significance is based on results from Student's T-tests pairwise comparisons where significance is $p < 0.05$.

**Table 1**

Length and volume changes by the distal phalanx after subjected to regenerating (<30%), intermediate (40–59%) or a non-regenerating (>60%) amputations. Data are expressed means ± S.E.M.

| | Ave. Length pre-amp. (mm) | Ave. Length post-amp. (mm) | Length Change (mm) | Percent Length Removed | Ave. vol. pre-amp (mm^3) | Ave. vol. post-amp (mm^3) | Percent Vol. Removed |
|---|---|---|---|---|---|---|---|
| **Regenerating** | 1.42 ± .02 | 1.18 ± .03 | 0.24 | 16.81 ± 1.53 | 0.20 ± .01 | 0.17 ± .004 | 12.34 ± 2.5 |
| **Intermediate** | 1.52 ± .01 | 0.77 ± .02 | 0.76 | 49.65 ± 1.31 | 0.29 ± .01 | 0.19 ± .01 | 32.70 ± 3.85 |
| **Non-Regenerating** | 1.49 ± .02 | 0.45 ± .02 | 1.04 | 69.92 ± 1.50 | 0.26 ± .01 | 0.11 ± .01 | 56.55 ± 4.11 |